

## PAPER

# Self-Routing Nonblocking WDM Switches Based on Arrayed Waveguide Grating\*

Yusuke FUKUSHIMA<sup>†</sup>, Student Member, Xiaohong JIANG<sup>†a)</sup>, Achille PATTAVINA<sup>††</sup>, Nonmembers, and Susumu HORIGUCHI<sup>†</sup>, Member

**SUMMARY** Arrayed waveguide grating (AWG) is a promising technology for constructing high-speed large-capacity WDM switches, because it can switch fast, is scalable to large size and consumes little power. To take the full advantage of high-speed AWG, the routing control of a massive AWG-based switch should be as simple as possible. In this paper, we focus on the self-routing design of AWG-based switches with  $O(1)$  constant routing complexity and propose a novel construction of self-routing AWG switches that can guarantee the attractive nonblocking property for both the wavelength-to-wavelength and wavelength-to-fiber request models. We also fully analyze the proposed design in terms of its blocking property, hardware cost and crosstalk performance and compare it against traditional designs. It is expected that the proposed construction will be useful for the design and all-optical implementation of future ultra high-speed optical packet/burst switches.

**key words:** self-routing, wavelength division multiplexing, strictly non-blocking, limited-range wavelength conversion

## 1. Introduction

With the deployment of Internet and in particular the wavelength division multiplexing (WDM) technology, many new network applications have emerged, such as the Grid computation, High Definition TeleVision, Cooperative Tele-Surgery, etc., and it is foreseeable that more such bandwidth-intensive applications will need to be supported in future networks. For the efficient support of these bandwidth-intensive applications, network switch, which serves as the switching core of network routers and cross-connects to implement the actual switching function, is expected to have the switch capability in the order of several Tbit/s or even Pbit/s.

Although the electronic switch/router technologies are mature and easy to implement, their capacity growth is historically slower than the growth of optical link capacity [1]. Also, the power consumption of network switch/router has exponentially increased beyond the standard acceptable level in past years [2]. This is why switches/routers have increasingly become a bottleneck for Internet com-

munications. Furthermore, the upgrade of current electronic switch/router solutions is becoming extremely costly and difficult due not only to the high costs of the optical-electronic-optical (O/E/O) conversions, but more importantly also to the strong dependence of switching hardware upon data bit-rate and transmission protocols. Therefore, some future alternative solutions for switch/router design are mandatory. A natural choice (also seems to be the only one) is to use all-optical switch/router. This is why there is a renewed interest in optical switch/router architectures, as evident from several ongoing national-scale projects in the US, Europe, and Asia, see, for example, [3]–[5]. Adopting optical switching can not only achieve over 100 Tbit/s or even Pbit/s throughputs [6], but also dramatically reduce the power consumption [1], eliminate the high cost O/E/O conversions and thus make the switching operation independent of bit-rate and protocol.

The arrayed waveguide grating (AWG)\*\* is a very attractive passive device for constructing high-speed large-capacity WDM optical switches, because it can switch fast, is scalable to large size, consumes little power and has less noise accumulation [7]. An AWG-based optical switch construction was proposed in [8] based on a single stage AWG. Even with the *full-range wavelength converters* (FWCs)\*\*\*, the design in [8] is still a blocking one. AWG-based nonblocking design is available in [9]. Although this architecture is simple and provides fast routing control, the higher hardware cost due to the large number of FWCs becomes impossible for the large size. Recently, the non-blocking designs of AWG-based optical switches for both the wavelength-to-wavelength and wavelength-to-fiber request models were investigated in [10] when the dedicated *limited-range wavelength converters* (LWCs) is adopted. This work was further extended in [9] when the shared wavelength conversion is adopted. It is notable, however, that in the available AWG switch designs, the routing control is complex because they need either to solve the combinatorial puzzle problem [8] or to apply the searching-based algorithms [9], [10] to reduce or avoid blocking. The high routing control complexity of current AWG switch designs can not fully realize the advantages offered by the high-

Manuscript received August 25, 2008.

Manuscript revised November 21, 2008.

<sup>†</sup>The authors are with the Graduate School of Information Sciences, Tohoku University, Sendai-shi, 980-8579 Japan.

<sup>††</sup>The author is with the Department of Electronics and Information, Politecnico di Milano, Italy.

\*This work was supported in part by JSPS grants (C) 19500050 and (B) 20300022, and the State Key Lab. on Integrated Service Networks, China.

a) E-mail: jiang@ecei.tohoku.ac.jp

DOI: 10.1587/transcom.E92.B.1173

\*\*AWG is wavelength sensitive and its switching speed is determined only by the speed of wavelength conversion, which is in the order of nanoseconds.

\*\*\*A FWC can convert any one of the incoming wavelengths into any other one of the outgoing wavelengths.

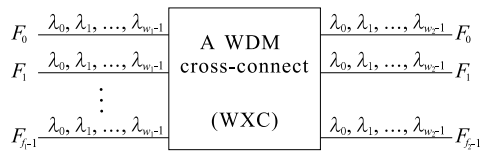


Fig. 1 A general WDM cross-connect.

speed AWG, so it may significantly degrade the switch performance/throughput.

In this paper, we explore another branch of AWG-based switches with the most simple routing control and LWCs, i.e. the self-routing AWG switches. Self-routing technique<sup>†</sup> is an attractive choice for reducing the routing complexity and achieving the constant routing complexity. We will show how to guarantee in a self-routing AWG switch the nice nonblocking property for the both the wavelength-to-wavelength and wavelength-to-fiber request models, and also devise solutions for a critical function module required by our design. The proposed design is compared with available ones in terms of complexity and crosstalk performance.

The rest of this paper is organized as follows. Section 2 introduces the preliminaries and an attractive nonblocking design of AWG-based switches proposed in [10]. Section 3 presents the overall construction of our AWG-based switch with both the self-routing capability and nonblocking guarantee, and also provide a possible design of a critical function module required in our switch design. In Sect. 4, our construction is compared with available ones in terms of construction components and routing complexity. We also compare their crosstalk performance in Sect. 5. Finally, Sect. 6 concludes this paper.

## 2. Preliminaries

The main notations to be used will be the same as that of [10], which motivates the work of this paper.

### 2.1 WDM Cross-Connect

A general “heterogeneous” WDM cross-connect (WXC) is illustrated in Fig. 1, with  $f_1$  input and  $f_2$  output fibers, each supporting  $w_1$  and  $w_2$  wavelengths, respectively, satisfying the condition  $f_1 w_1 = f_2 w_2$ . Without loss of generality, in this paper we just focus on the “homogeneous” WXC constructions in which  $f = f_1 = f_2$  and each fiber carries same set of  $w = w_1 = w_2$  wavelengths. We use  $\Lambda = \{\lambda_0, \lambda_1, \dots, \lambda_{w-1}\}$  to denote the set of these  $w$  wavelengths and use  $F$  and  $F'$  to denote the set of input fibers and the set of output fibers, respectively. Let  $A$  and  $B$  be two wavelength subsets of  $\Lambda$ , then the wavelength converter (WC) that converts any wavelength in  $A$  to any wavelength in  $B$  will be denoted by  $WC(A, B)$ . Especially, the wavelength converter that can convert a signal to one of the wavelength in  $\Lambda$  is referred to as FWC. For example, FWC can be expressed as  $WC([1], \Lambda)$ ,  $WC(\Lambda, [1])$  or  $WC[\Lambda, \Lambda]$ . We also define  $[i, j]$  as a subset of  $(j - i)$  wavelengths  $\{\lambda_i, \lambda_{i+1}, \dots, \lambda_{j-1}\}$ , and

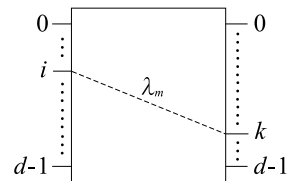


Fig. 2 A  $d \times d$  AWG router.

define  $[0, j] = [j]$  for short.

In current AWG-based nonblocking WXC designs, two different request models have been mainly considered [9], [10], namely the  $(\lambda, F, \lambda', F')$  and  $(\lambda, F, F')$  request models. In the  $(\lambda, F, \lambda', F')$ -request model, an input signal carried on a wavelength  $\lambda \in \Lambda$  from an input fiber  $F \in F$  is destined for a specified wavelength  $\lambda' \in \Lambda$  on an output fiber  $F' \in F'$ . As wavelength-to-wavelength switching is required under this request model, this model is suitable for circuit switching and quality of service (QoS) guarantees. In the  $(\lambda, F, F')$ -request model, the only difference is that output wavelength of this request is not specified and can be any free wavelength in output fiber  $F' \in F'$ . This model requests more general fiber-to-fiber switching and is more suitable for optical burst/packet switching.

### 2.2 Arrayed Waveguide Grating Routers

The arrayed waveguide grating router (AWGR) is an attractive passive wavelength routing device that consumes almost no power, has less noise accumulation and can switch very fast (only through wavelength conversion)[7]. In an AWGR, the routing of an input signal is solely determined by its wavelength and input port address. For a  $d \times d$  AWGR illustrated in Fig. 2, an incoming optical signal carried on the wavelength  $\lambda_m \in [d]$  in the  $i$ -th input will always be switched to a given output port  $k$  on the same wavelength, where  $k$  is given by

$$k = (m - i + d) \bmod d \quad (1)$$

where  $m \geq 0$  and  $i, k < d$ . From the above equation we can easily see that in an AWGR a signal in any input port can actually reach any output port by properly controlling its wavelength  $\lambda_m$ .

### 2.3 Nonblocking AWG-Based Switches

#### 2.3.1 SNB WXC with Three-Stage LWCs

By emulating the well-known Clos switch architecture [11], a novel AWG-based switch design was proposed in [10] to provide the strictly nonblocking (SNB) guarantee for both the  $(\lambda, F, \lambda', F')$  and  $(\lambda, F, F')$  request models. One such SNB design is illustrated in Fig. 3 for the case when  $f = 2$

<sup>†</sup>By self-routing we mean that for a connection request we can determine a unique routing path based only on its input/output addresses.

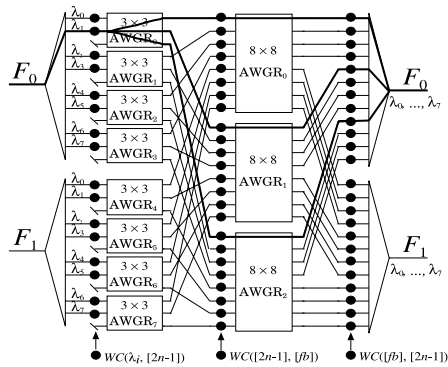


**Fig. 3** An SNB-WXC2 construction, where  $f = 2, w = 8, n = 2, b = 4$ . Three paths are available for each request.

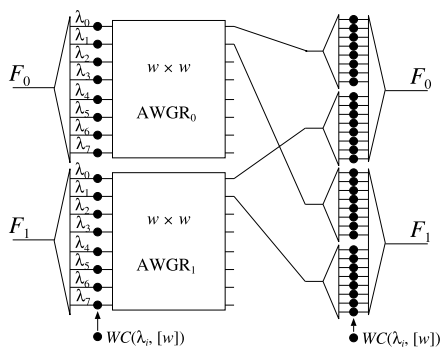


**Fig. 4** An example of multi- $\lambda$  construction, where  $f = 2, w = 8$ .

and  $w = 8$ . We can see from the Fig. 3 that this design consists of limited-range wavelength converters (LWCs) and two-stage of AWGRs, where the second-stage of AWGRs just corresponds to the middle stage of a Clos switch. It is notable that in the above Clos-like design of AWGR-based switch, multiple routing paths are available for each input-output pair. For the example shown in Fig. 3, all the three paths for the request  $(\lambda_1, F_0, \lambda_1, F_0)$  are highlighted. Since the routing path for a request is not fixed and must be selected among one of  $2n-1$  second-stage AWGRs (here  $n = 2$  and  $2n-1$  is the size of first stage AWGR [10], and  $n$  is given by  $w/b$ ), so the worst routing complexity can be as high as  $O(nfw)$  for both request models. This routing complexity of above designs increases with both the switch size  $fw$  and parameter  $n$ . This high routing control complexity will not only significantly degrade the performance/throughput of current AWG-based switch designs, but also make the all-optical implementation impractical for the future massive WDM switches.

### 2.3.2 SNB WXC with Two-Stage FWCs

A traditional single stage SNB AWG-based WXC switch architecture, namely the multi- $\lambda$  switch was proposed in [9] and shown in Fig. 4. The architecture consists of a single stage of AWGRs, two stages of wavelength converters and a set of demultiplexers in the middle stage. Such demultiplexers are referred to as the *middle demultiplexer*. AWGRs

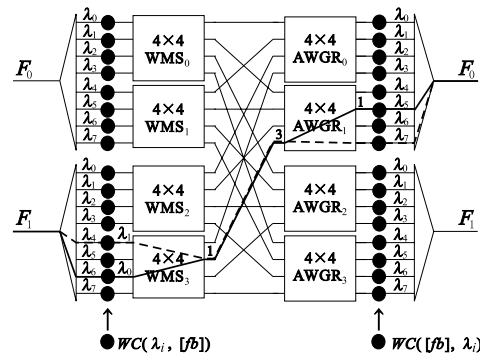


**Fig. 5** An example of proposed construction, where  $f = 2, b = 2, n = 4$ .

corresponding to the input fibers work as the selector of output fibers, and the middle demultiplexer after the AWGR demultiplex input signals according to their wavelength. Finally, a dedicated FWC at the second stage can convert an input signal to an any wavelength available at the output port. Since there always exists one routing path for given input and output ports, the multi- $\lambda$  switch has self-routing capability. Thus, the routing control of this design is very simple and can achieve  $O(1)$  fast parallel routing due to its SNB and self-routing capability; However, the large number of FWCs at the second stage implies high cost for building large size WXC, since FWC has higher cost than LWC.

## 3. A New Self-Routing and Nonblocking Design of AWGR-Based Switch

In this section, we propose a self-routing design of AWG-based switch that has the constant routing complexity and can still provide the nonblocking guarantee for both the  $(\lambda, F, \lambda', F')$  and  $(\lambda, F, F')$  request models.

### 3.1 Construction Overview

The main idea of our proposed AWG switch design is inspired by the Spanke switch architecture [12], which is well-known as a self-routing and nonblocking architecture. For an AWG-based switch that supports  $f = 2$  input (output) fibers with  $w = 8$  wavelengths each, one sample construction of the proposed self-routing design is illustrated in Fig. 5 and Fig. 6. In the proposed construction, the  $w$  wavelengths of each fiber are partitioned into  $b$  consecutive bands each with size  $n$ . All the  $\lambda$ s in one band, each controlled by a  $WC(\lambda, [fb])$ , are inputs to an  $n \times n$  special module in the first stage, referred to as the “wavelength multiplexing switch” (WMS). The second stage of the design consists of  $n$  AWGRs of size  $fb \times fb$ , followed by a  $WC([fb], \Lambda)$  in each output port. All the WMSs and AWGRs in the design are continuously numbered from  $WMS_0$  to  $WMS_{fb-1}$  and from  $AWGR_0$  to  $AWGR_{n-1}$ , respectively.

In the proposed design, the main function of the special WMS module is to guarantee that any set of distinct wavelengths at any set of its distinct input ports can be simultaneously routed to any common output port. This function

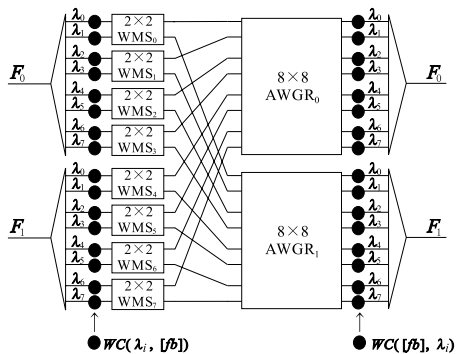


Fig. 6 Another configuration of the proposed construction, where  $f = 2$ ,  $b = 4$ ,  $n = 2$ .

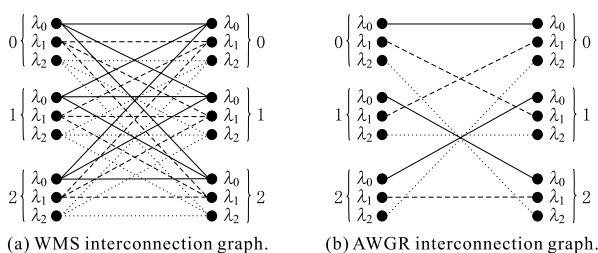


Fig. 7 Connectivity comparison between WMS and AWGR.

also implies that a given wavelength at a given input port can be freely routed to any output port. One possible design of WMS will be introduced in Section IV to provide the above function. We should note that the function requirement of WMS is much stronger than its AWGR counterpart, since in AWG a given wavelength at a given input port can only be routed to a fixed output port. The connectivity difference between WMS and AWGR is further illustrated in Fig. 7 for the case of  $f = 3$  and  $w = 3$ . It is worth noting that our two-stage design makes it possible to control the overall complexity of the WMS module, since we can properly select its size ( $n$ ) to make it suitable to the available technology. A single-stage solution would require necessarily a single WMS whose dimension ( $fw$ ) is only determined by external parameters.

In addition to the new and more powerful WMS, the new switch design also explores both the WDM property of the central links and the splitting function of AWGRs, since in our design each central link now can simultaneously multiplex wavelengths and each AWGR at second stage can automatically split these multiple WDM signals carried in the central links in a same way as a passive splitter (please refer to Fig. 5 for the routing of two connections  $(\lambda_6, F_1, \lambda_5, F_0)$  and  $(\lambda_4, F_1, \lambda_7, F_0)$ ). These nice properties, as far as we know, were not fully explored in available SNB designs of AWG-based switches [9], [10].

In the next two subsections, we will show that based on the new WMS module and thanks to the above two properties, our design is able to provide both the self-routing and nonblocking (SNB) guarantees for the  $(\lambda, F, \lambda', F')$  and  $(\lambda, F, F')$  requests.

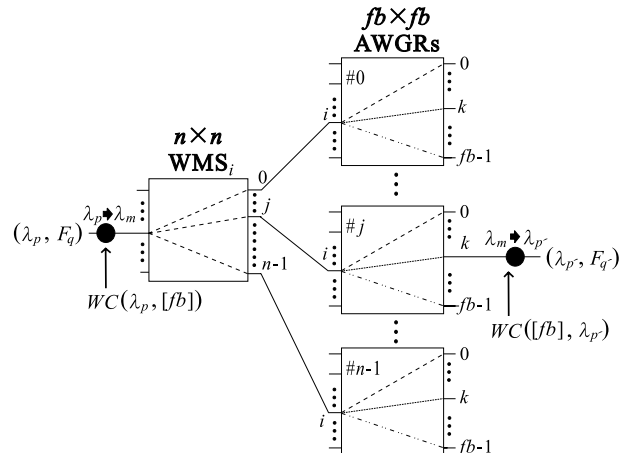


Fig. 8 Connection pattern between WMS<sub>*i*</sub> and AWGRs.

### 3.2 Self-Routing Guarantee

In this section, we will show that the proposed design has the self-routing capability for  $(\lambda, F, \lambda', F')$ -request model i.e. it can determine a unique path (i.e., lightpath) for such a request based only on its input address  $(\lambda, F)$  and output address  $(\lambda', F')$ .

**Theorem 3.1:** The proposed design provides self-routing capability for any  $(\lambda, F, \lambda', F')$  request.

*Proof.* For a tagged request in the form of  $(\lambda_p, F_q, \lambda_{p'}, F_{q'})$ , we will first prove that only one unique path is available for it and then show how to determine the path based on its input and output addresses only.

Suppose that the input port of  $(\lambda_p, F_q)$  is associated with WMS<sub>*i*</sub> in the first stage and the  $(\lambda_{p'}, F_{q'})$  is associated with the output port  $k$  of AWGR<sub>*j*</sub> in the second stage, then the connection pattern between WMS<sub>*i*</sub> and all  $n$  AWGRs (including the AWGR<sub>*j*</sub>) is illustrated in Fig. 8. We can see easily from the Figure that the only central link between WMS<sub>*i*</sub> and AWGR<sub>*j*</sub> is the one that connects the  $j$ -th output of WMS<sub>*i*</sub> to the  $i$ -th input of AWGR<sub>*j*</sub>. Of course, to prove that for the tagged request only unique path is available between WMS<sub>*i*</sub> and AWGR<sub>*j*</sub>, we need to show that the wavelength that can be used for it is also unique. Notice that from the  $i$ -th input to the destined  $k$ -th output of AWGR<sub>*j*</sub>, only a unique wavelength (and thus a unique path) is available due to the wavelength-based switching property of AWGR. Suppose this unique wavelength is  $\lambda_m$ . Since no wavelength conversion capability is available between the WMS stage and AWGR stage, so for the tagged request the only wavelength (and thus the only path) that can be used between WMS<sub>*i*</sub> and AWGR<sub>*j*</sub> is just  $\lambda_m$ . Thus, for the tagged request only a unique path is available through the proposed switch design.

The routing indices  $i$ ,  $j$  and  $k$  for the tagged request can be easily determined from the architecture of proposed design. For example, the index  $i$  is defined as

$$i = bq + \lfloor p/n \rfloor \quad (2)$$

Similarly, let  $n' = fb$  and  $b' = w/fb$ , so that  $j$  will be defined as

$$j = b'q' + \lfloor p'/n' \rfloor \quad (3)$$

The index  $k$  is then uniquely defined by  $j$  and  $\lambda_{p'}$  (please refer to Fig. 5). From the indices  $i$  and  $k$ , the wavelength index  $m$  of the tagged request will be uniquely determined by the following formula based on the routing property of AWGR in (1)

$$m = (i+k) \bmod (fb) \quad (4)$$

□

From the above proof we can see that to route a connection  $(\lambda_p, F_q, \lambda_{p'}, F_{q'})$ , it first needs to go through the first stage LWC, which converts its wavelength  $\lambda_p$  into  $\lambda_m$  and routes it to the  $WMS_i$  based on the architecture of the proposed design. Based on its output address  $(\lambda_{p'}, F_{q'})$ , the  $WMS_i$  routes it to  $AWGR_j$  through the unique link between them. The  $AWGR_j$  then automatically route this signal to its destined output port  $k$  based on its input port number  $i$  and its wavelength  $\lambda_m$ . Finally, this signal is converted to its destined wavelength  $\lambda_{p'}$  by the second stage LWC. For example, for two requests  $(\lambda_6, F_1, \lambda_5, F_0)$  and  $(\lambda_4, F_1, \lambda_7, F_0)$ , their routing is illustrated in Fig. 5.

It is notable that the routing complexity of any  $(\lambda, F, \lambda', F')$  request is just  $O(1)$ , since its route is simply determined by Eqs. (2), (3) and (4) only.

### 3.3 Nonblocking Guarantee

In this section, we further show that the proposed design is also nonblocking (strictly nonblocking) for wavelength-to-wavelength request model

**Theorem 3.2:** The proposed construction is nonblocking under  $(\lambda, F, \lambda', F')$ -request model.

*Proof.* To guarantee the nonblocking property under the  $(\lambda, F, \lambda', F')$  model, we just need to show that for any two different  $(\lambda, F, \lambda', F')$  requests (with different input address  $(\lambda, F)$  and also different output address  $(\lambda', F')$ ), blocking will never happen along their paths. First, blocking can not happen at their input/output ports, since each  $(\lambda, F)$  pair (correspondingly  $(\lambda', F')$  pair) has its dedicated input port (output port) as defined by the switch architecture itself. Second, blocking in a WMS module can not happen between these two requests, i.e., they can not be routed to the same output of the WMS on a same wavelength. Otherwise, these two requests will be forwarded to a common input of a AWGR on the the same wavelength and will be finally routed to the same output address (notice the output addresses of these two requests can not be same). Finally, blocking can not happen at the AWGR stage, since two signals of same wavelength can neither be routed to a common input of an AWGR as guaranteed by the preceding WMS

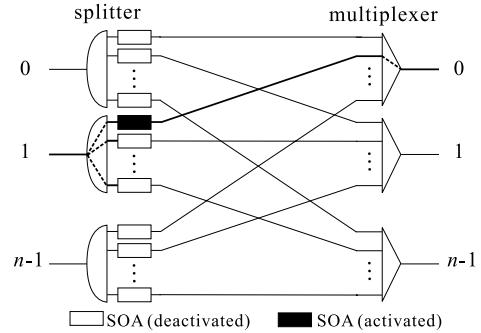


Fig. 9 A construction of  $n \times n$  WMS with splitters and SOAs.

stage nor routed to a common output port as assured by the routing property (1) of AWGR. □

We can see easily from above proof that for any two different  $(\lambda, F, \lambda', F')$  requests, their paths never share any common link/wavelength pair, so the routing of a new request is completely independent from other connections. Thus, the proposed design actually provides the strictly non-blocking guarantee for  $(\lambda, F, \lambda', F')$  request.

### 3.4 Wavelength Multiplexing Switch (WMS)

In this section, we propose a splitter-based design of the WMS module adopted in our switch architecture. The combination of optical splitter and semiconductor optical amplifier (SOA) is an attractive approach to building high-speed but small size switch, because a connection can be switched ON or OFF in nanosecond by using only single SOA [13], [14]. A  $n \times n$  WMS design based on the splitter and SOA is shown in Fig. 9, where an incoming signal is split into  $n$  signals by an input-side splitter. The switch function is then controlled by the SOA, since each signal is routed to an output only when the corresponding SOA is activated, otherwise this signal will be dropped (blocked). It is notable that the above splitter-based construction of WMS essentially supports the multicast transmission capability. How to explore this capability to design the self-routing and multicast optical switch remains to be explored further.

## 4. Complexity Comparison

In this section, the proposed switch design will be compared with the available AWGR-based SNB designs [9], [10] in terms of both hardware and routing control complexities. The comparison results are summarized in Table 1, where  $x \otimes y$  means  $x$  elements (AWGR or WMS) of size  $y \times y$  each.

For the hardware requirement between WXC-SNB2 and the proposed design, we can see from Table 1 that the LWC complexity of available AWGR-based SNB design in [10] is at least 1.5 times as that of the new design given that  $w \gg b$  in normal cases, while its AWGR complexity is about 3 times as that of the new one. Although the new design requires the WMSs with complexity  $fb \otimes n$ , its overall construction complexity can be even lower than the avail-

**Table 1** Comparison of hardware and routing complexities of different architectures.

	Switch components					Routing complexity	
	#FWCs	#LWCs	#AWGRs	#WMSs	#MUXs	$(\lambda, F, F')$	$(\lambda, F, \lambda', F')$
Multi- $\lambda$ Switch[9]	$f^2w+fw$	–	$f \otimes w$	–	$(f+f^2) \otimes w, f \otimes fw$	$O(1)$	$O(1)$
WXC-SNB2 [10]	–	$5fw - 2fb$	$fb \otimes n, 2n - 1 \otimes fb$	–	$2f \otimes w$	$O(nfw)$	$O(nfw)$
Proposed	–	$2fw$	$n \otimes fb$	$fb \otimes n$	$2f \otimes w$	$O(1)$	$O(1)$

able design if an efficient design of WMS is adopted. The splitter-based WMS components may be expensive because each of  $fb$  WMSs consists of  $n^2$  SOAs (total  $fbn^2$  SOAs), and cost of the WMS cannot be compared exactly with other switch components. Although the most of wavelength converters is based on SOA technology [15], the most expensive part of wavelength converter is other tunable components such as a tunable laser. Hence, LWC is less expensive than FWC [10], [16], and the relation of the hardware cost among a single SOA, LWC and FWC can be given as  $SOA < LWC < FWC$ . Thus, a suitable  $n$  can be found to minimize total cost of the proposed design according to current technology, and we believe that the proposed WXC can be less expensive than multi- $\lambda$  switch.

For routing control complexity, the proposed self-routing design and multi- $\lambda$  switch clearly outperform the WXC-SNB2 (see Table 1). Since in the AWGR-based SNB design [10], the sequential searching process may need to find the routing path for a request, this could result in a worst complexity as high as  $O(nfw)$ , while the proposed design and multi- $\lambda$  switch can always guarantee a constant routing complexity under both  $(\lambda, F, \lambda', F')$  and  $(\lambda, F, F')$  request models.

## 5. Crosstalk Performance

For any optical components, there are some leakage optical power from the input to the undesired output ports due to imperfections of the optical components. This signal leakage is referred to as crosstalk and results in the additive noise for other signals. The crosstalk is classified into the outband and the inband crosstalk. Although the former can be additive noise with different wavelength of the main signal, the crosstalk power can be easily removed by employing filters. This crosstalk is also referred to as incoherent crosstalk. The latter can be major source of crosstalk contributions, because this kind of crosstalk can be additive noise with the same wavelength of the main signal. This type of crosstalk is also referred to as coherent crosstalk.

For practical WXC designs, power penalty (PP) of the inband crosstalk is also useful measurement of the switch performance [17]–[22]. We study the PP of the traditional and the proposed SNB WXC designs here.

### 5.1 Crosstalk Contributions

**AWGR:** The crosstalk contribution of AWGR consists of the adjacent and non-adjacent crosstalks. The former is contributed from adjacent input ports of the main signal, and the

latter is contributed from other input ports. Let  $\delta_m$ ,  $\delta'_a$  and  $\delta'_n$  denote optical powers related to a total, an adjacent and non-adjacent crosstalk contributions for  $m \times m$  AWGR, respectively. The total crosstalk contribution can be expressed as [23].

$$\delta_m = \min(2, m-1)\delta'_a + \max(0, m-3)\delta'_n \quad (5)$$

Although  $\delta'_n$  is usually much less than  $\delta'_a$ ,  $\delta'_n$  becomes dominant crosstalk contribution as the number of inputs/outputs of AWGR increases. It is notable that there is also the leakage of  $\delta_m$  from the main signal to the other outputs.

**WMS:** We consider the crosstalk contributions in the splitter-based WMS switch. Although the optical power of input signal is split into the number of output port, each signal amplitude can be amplified by an SOA with ON-state. In the splitter and SOA based switch, one amplified signal is transmitted to output port, while other signals are not transmitted with OFF-state. Due to imperfect isolation of OFF-state, the crosstalk signal can be generated and coupled at the multiplexer at output of the WMS. Assume that the initial noise and the amplified spontaneous emission (ASE) noise is neglected [22]. Let  $\gamma$  denote a crosstalk contribution related to the main signal, so the total crosstalk power for a  $m' \times m'$  WMS can be expressed as

$$\sum_{i=2}^{m'} \gamma = (m' - 1)\gamma. \quad (6)$$

**Filter:** Let  $\epsilon$  and  $\epsilon'$  denote the crosstalk contributions of the fixed-range and the tunable-range filter related to the main signal, respectively. The former pass optical signal in fixed pass-band, while the latter can change the pass-band by electrical control. Thus,  $\epsilon$  may be little smaller than  $\epsilon'$ . Due to imperfect isolations, there are also leakages from a filter. Consider only leakage from adjacent wavelengths ( $\omega' \pm 1$ ) as the dominant crosstalk contribution [20], [22], where  $\omega'$  is the central wavelength of the input signal.

### 5.2 Crosstalk Evaluation

To calculate the inband crosstalk behavior of the proposed WXC design, we follow an approximation approach of [20]. We consider intensity modulation system, and assume that all noise process are Gaussian and the laser coherence time is less than the delay of crosstalk signal relative to the main signal. The electric field with the center frequency  $\omega$  of  $i$ -th input is given by  $\vec{E}_0(t) = Eb_i(t) \cos[\omega t - \phi_i(t)] \vec{P}_i$ , where  $E$ ,  $b_i(t)$ ,  $\phi_i(t)$  and  $\vec{P}_i$  are the signal field amplitude, the binary sequence with value of 0 or 1 in the bit period  $T$ , the

**Table 2** Notations.

$E$	Signal field amplitude
$ \vec{E}_0(t) $	Electrical field of the main signal when there is no crosstalk.
$ \vec{E}(t) $	Electrical field of the main signal when there is no crosstalk.
$b_i$	Binary sequence with value of 0 or 1 in the bit period $T$ from $i$ -th input of switch component.
$P_i$	Unit polarization vector of the signal from $i$ -th input of switch component.
$r$	Extinction ratio of the main signal.
$\omega$	Center frequency of signal.
$\phi_i(t)$	Phase noise of the laser.
$\tau_i$	Propagation delay from $i$ -th input of switch component.
$\gamma$	Optical power related to a crosstalk contribution for WMS.
$\delta_m, \delta'_a, \delta'_n$	Optical power related to a total, an adjacent and a non-adjacent crosstalk contributions for $m \times m$ AWGR, respectively.
$\epsilon, \epsilon'$	Optical power related to a crosstalk contribution for the fixed-range and the tunable-range filters, respectively.

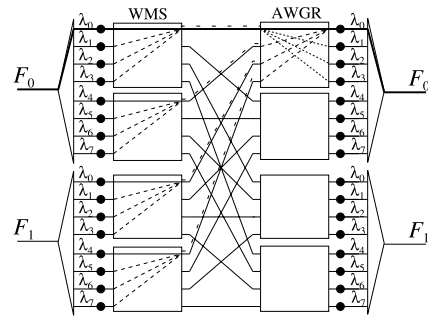
phase noise of the laser and the unit polarization vector of the signal, respectively. When the photodetector at output of OXC uses an integrate-and-dump filter, the decision variable is  $J = \int_{kT}^{(k+1)T} |\vec{E}(t)|^2 / |\vec{E}_0(t)|^2 dt$ , where  $\vec{E}_0(t)$  is the electrical field of the main signal when there is no crosstalk,  $k$  is an arbitrary integer. For  $J$ , crosstalk power penalty (PP) is given by [20]

$$PP = -10 \log_{10} \left\{ E(J)^2 - 4\sigma^2 Q^2 \left( \frac{r}{r-1} \right)^2 \right\}, \quad (7)$$

where  $E(J)$  and  $\sigma^2$  are mean and variance of  $J$ , respectively.  $Q$  is obtained from  $BER = 1/4 \cdot \text{erfc}(Q/\sqrt{2})$ , and  $r$  is the extinction ratio. For practical BER of  $10^{-9}$ ,  $Q = 5.9$  and  $r = 20$ . In the following PP calculations, we assume that all switch construction shown in this paper is fully loaded. All the notations defined in this section are summarized in Table 2.

### 5.2.1 Power Penalty Calculation

(1) Proposed Design: The worst case crosstalk scenario of the proposed design for a request  $(\lambda_0, F_0, \lambda_0, F_0)$  is shown in Fig. 10. The bold and dash lines illustrate the main signal and crosstalk signals, respectively. As we can see, a number of crosstalk contributions from the different source are coupled at the output. In this case, the electrical field of the main signal and all the crosstalk contributions can be expressed by (9) at the bottom of the next page, where  $\tau_i$  is the propagation delay from  $i$ -th input of a switch component. The first term of (9) is the field amplitude of the main signal with loss  $\delta_{fb}$ . The second term is the field amplitude of the WMS, and the third and the four-th terms are of the crosstalk at AWGR. The last term is of single filters. It is notable that


**Fig. 10** The worst case crosstalk scenario of the proposed SNB-WXC design.

the inband crosstalk contributions from filters can be only two sources, because the output wavelength of the 2nd stage LWC is dedicated for each output port. From (9), by using approximation in [20],  $J$  can be given by (10) at the bottom of the next page. The mean and the maximum variance of  $J$  can be obtained approximately as

$$E(J) = 1 - \delta_{fb}$$

$$\sigma^2 = \frac{2}{3}(1 - \delta_{fb})[(n-1)\gamma + \delta_{fb} + 2\epsilon] \quad (8)$$

From (8) and (7), the PP is given by

$$PP = -10 \log_{10} \left\{ (1 - \delta_{fb})^2 - \frac{8}{3}(1 - \delta_{fb}) \cdot \right.$$

$$\left. \times [(n-1)\gamma + \delta_{fb} + 2\epsilon] Q^2 \left( \frac{r}{r-1} \right)^2 \right\}$$

(2) SNB-WXC2 Design [10]: The SNB-WXC2 shown in Fig. 3 consists of 2-stage AWGRs and output tunable filters. As we mentioned in Sect. 2.3.1, there are  $2n-1$  choices of routing path for  $(\lambda, F, \lambda', F')$ -request model. Hence, there are  $2n-2$  inband crosstalk contributions generated from tunable filters can be coupled with the main signal at the final multiplexer. In the same way as the proposed design, the electrical field of the main signal and all the crosstalk contributions can be expressed as (11) at the bottom of the this page. By calculating (11) in the same way as the proposed design, the mean and the maximum variance of  $J$  with (11) is approximately given by

$$E(J) = (1 - \delta_{2n-1})(1 - \delta_{fb})$$

$$\sigma^2 = \frac{2}{3}(1 - \delta_{fb})^2 \left[ \delta_n(1 - \delta_{fb}) + \delta_{fb} + 2(n-1)\epsilon' \right] \quad (13)$$

(3) Multi- $\lambda$  Design [9]: The multi- $\lambda$  shown in Fig. 4 consists of the single stage AWGRs and output tunable filters. As we can see in Sect. 2.3.2, since there is a number of links connected from AWGRs to each output multiplexer, a large number of inband crosstalk contributions can be coupled with the main signal at the output multiplexer. There are two crosstalk contributions from the same middle demultiplexer of the main signal, and there are three crosstalk contributions from a different middle demultiplexer. Thus,

in the same way as the proposed design, the electrical field of the main signal and all the crosstalk contributions can be expressed as (12) at the bottom of the this page. Based on (12), the mean and the maximum variance of  $J$  with (12) is approximately given by

$$E(J) = 1 - \delta_w$$

$$\sigma^2 = \frac{2}{3}(\delta_w + (3f - 1)\epsilon')$$
(14)

### 5.2.2 Power Penalty Comparison

Consider  $f = 10$ ,  $w = 50$ ,  $\epsilon = \epsilon'$  and the acceptable PP = 2 dB. Since constructing WXC with large size on dense WDM (DWDM) networks is needed, PP calculation with the large number of wavelengths is useful, because 50–70 transmitted channels on a fiber are available based on ITU-T spectral grid for DWDM (G.694.1). It is notable that 10 neighbors are large enough number of input/output fibers compared with available literature [17], [19], [20], and PP calculation with above parameters are useful to observe crosstalk performance of large size WXC components on DWDM networks. In the worst crosstalk scenario,  $\epsilon'$  can be equal to  $\epsilon$  because the fixed-range filter usually achieve better signal isolation than tunable one. Additionally, the routing control of WXC-SNB2 is at least 2,000 times more complex than the proposed design and multi- $\lambda$  switch because  $n$  should be larger than 2 for WXC-SNB2 design.

Figure 11 illustrates the PP against the number of input ports of the 1st stage switch component, where  $\epsilon = -40$  dB,  $\delta'_a = -40$  dB and  $\delta'_n = -50$  dB. Although an adjacent and non-adjacent crosstalk of practical AWGR are  $-30$  dB and  $-40$  dB, respectively, above better crosstalk parameters

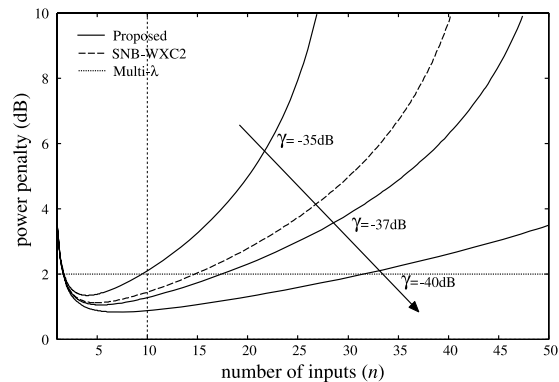


**Fig. 11** Power penalty versus 1st stage switch size and crosstalk of the WMS component, where  $f = 10$  and  $w = 50$ .

of AWGR give useful observation for near future DWDM applications because current crosstalk reduction technique of AWGR can achieve total adjacent crosstalk estimated  $-34$  dB [23], thus  $\delta'_a$  can be  $-40$  dB, and a non-adjacent crosstalk is usually less than an adjacent crosstalk. Figure 11 also include the PP of the proposed design with different values of  $\gamma$  from  $-35$  dB to  $-40$  dB. Since wavelength conversion range is limited from 0 to  $w-1$ ,  $n$  may be larger than 9 for the above configuration ( $f = 10$  and  $w = 50$ ). It is interesting to see that the PP of the proposed design is less than others even when  $\gamma$  is equal to  $\delta'_a$  ( $\gamma = -40$  dB). Figure 12 further illustrates the PP for different values of the  $\epsilon$  from  $-38$  dB to  $-42$  dB and with  $\gamma = -37$  dB. As we can see, the  $\epsilon$  can significantly affect the PP of traditional designs, while it is not sensitive to the proposed design. Figure 13 illustrates that the relation between the  $\epsilon$  and the  $\delta'_n$  with  $\delta'_a = -40$  dB

$$\vec{E}(t) = \sqrt{1 - \delta_{fb}} E b_1(t) \cos[\omega t - \phi_1(t)] \vec{P}_1 + \sum_{i=2}^n \sqrt{\gamma} E b_i(t) \cos[\omega(t - \tau_i) - \phi_i(t - \tau_i)] \vec{P}_i$$

$$+ \sum_{j=2}^3 \sqrt{\delta'_a} E b_j(t) \cos[\omega(t - \tau_j) - \phi_j(t - \tau_j)] \vec{P}_j + \sum_{j=4}^{fb} \sqrt{\delta'_n} E b_j(t) \cos[\omega(t - \tau_j) - \phi_j(t - \tau_j)] \vec{P}_j + \sum_{s=1}^2 \sqrt{\epsilon} E b_s(t) \cos[\omega(t - \tau_s) - \phi_s(t - \tau_s)] \vec{P}_s$$
(9)

$$J \approx \frac{\sqrt{1 - \delta_{fb}}}{T} \left\{ \int_{kT}^{(k+1)T} b_1^2(t) dt + 2 \sum_{i=2}^n \sqrt{\gamma} \int_{kT}^{(k+1)T} b_1(t) b_i(t - \tau_i) \cos[\phi_1(t) - \phi_i(t)] dt \cdot \cos \theta_i \right.$$

$$\left. + 2 \left( \sum_{j=2}^3 \sqrt{\delta'_a} \int_{kT}^{(k+1)T} b_1(t) b_j(t - \tau_j) \cos[\phi_1(t) - \phi_j(t)] dt \cdot \cos \theta_j \right. \right.$$

$$\left. + \sum_{j=4}^{fb} \sqrt{\delta'_n} \int_{kT}^{(k+1)T} b_1(t) b_j(t - \tau_j) \cos[\phi_1(t) - \phi_j(t)] dt \cdot \cos \theta_j \right) + 2 \sum_{s=1}^2 \sqrt{\epsilon} \int_{kT}^{(k+1)T} b_1(t) b_s(t - \tau_s) \cos[\phi_1(t) - \phi_s(t)] dt \cdot \cos \theta_s \left. \right\}$$
(10)

$$\vec{E}(t) = \sqrt{(1 - \delta_{2n-1})(1 - \delta_{fb})} E b_1(t) \cos[\omega t - \phi_1(t)] \vec{P}_1 + \sqrt{1 - \delta_{fb}} \left( \sum_{i=2}^n \sqrt{\delta'_a} E b_i(t) \cos[\omega(t - \tau_i) - \phi_i(t - \tau_i)] \vec{P}_i \right.$$

$$\left. + \sum_{i=2}^n \sqrt{\delta'_n} E b_i(t) \cos[\omega(t - \tau_i) - \phi_i(t - \tau_i)] \vec{P}_i \right) + \sum_{j=2}^3 \sqrt{\delta'_a} E b_j(t)$$

$$\times \cos[\omega(t - \tau_j) - \phi_j(t - \tau_j)] \vec{P}_j + \sum_{j=4}^{fb} \sqrt{\delta'_n} E b_j(t) \cos[\omega(t - \tau_j) - \phi_j(t - \tau_j)] \vec{P}_j + \sum_{s=1}^{2(n-1)} \sqrt{\epsilon'} E b_s(t) \cos[\omega(t - \tau_s) - \phi_s(t - \tau_s)] \vec{P}_s$$
(11)

$$\vec{E}(t) = \sqrt{(1 - \delta_w)} E b_1(t) \cos[\omega t - \phi_1(t)] \vec{P}_1 + \sum_{j=2}^3 \sqrt{\delta'_a} E b_j(t) \cos[\omega(t - \tau_j) - \phi_j(t - \tau_j)] \vec{P}_j + \sum_{j=4}^{fb} \sqrt{\delta'_n} E b_j(t) \cos[\omega(t - \tau_j) - \phi_j(t - \tau_j)] \vec{P}_j$$

$$+ \sum_{s=1}^{2(n-1)} \sqrt{\epsilon'} E b_s(t) \cos[\omega(t - \tau_s) - \phi_s(t - \tau_s)] \vec{P}_s$$
(12)

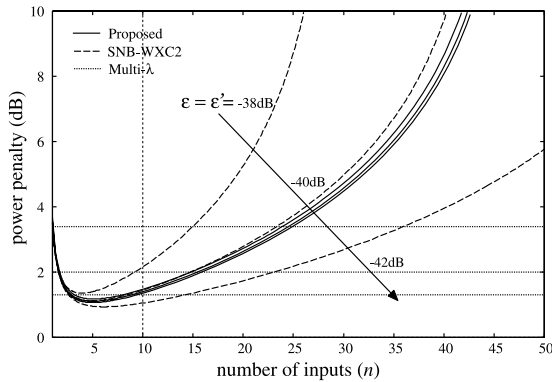


**Fig. 12** Power penalty versus crosstalk of the filter, where  $f = 10$  and  $w = 50$ .

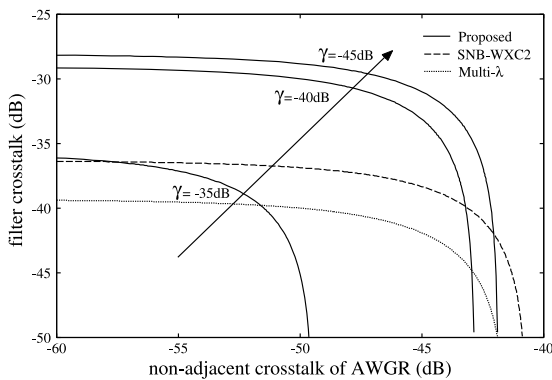


**Fig. 13** Required filter crosstalk relative to the  $\delta'_n$  when  $pp = 2$  dB,  $fb = w$  and  $\delta'_a = -40$  dB.

when  $n = 10$  and  $PP = 2$  dB. This comparison is useful, because  $\delta'_n$  is dominant for the total crosstalk of AWGR [23]. Figure 13 also include the result of the proposed design with different value of the  $\gamma$  from  $-35$  dB to  $-45$  dB. It can be observed that the proposed design has trade-off between  $\gamma$  and both  $\delta'_n$  and  $\epsilon$ . For example, if either  $\epsilon$  or  $\delta'_n$  is small, the larger  $\gamma$  may be acceptable and vice versa.

**6. Conclusion**

In this paper, we have proposed a self-routing and also strict nonblocking (SNB) design of optical switch with limited-range-wavelength converters for both wavelength-to-wavelength and wavelength-to-fiber request models. We have showed that despite its self-routing and nonblocking guarantees, the overall construction complexity of the proposed design is lower than that of the current AWG-based SNB switch design. We also studied the crosstalk performance for the proposed design and other traditional designs. One possible future work is to find a more cost effective design for the wavelength multiplexing switch (WMS) module adopted in our construction.

**References**

[1] I. Keslassy, S. Chuang, K. Yu, D. Miller, M. Horowitz, O. Solgaard,

and N. McKeown, "Scaling Internet routers using optics," Proc. ACM SIGCOMM 2003, Karlsruhe, Germany, 2003.

[2] C. Minkenber, R. Luijten, F. Abel, W. Denzel, and M. Gusat, "Current issues in packet switch design," Computer Communication Review, vol.33, no.1, pp.119–124, Jan. 2003.

[3] ARNGNC Project, <http://gibbs.ee.nthu.edu.tw:80/top/>

[4] LASOR Project, <http://www.ia.ucsb.edu/pa/display.aspx?pkey=1136>

[5] OSATE Project, <http://www1.tlc.polito.it/projects/osate/>

[6] H. Chao, K. Deng, and Z. Jing, "PetaStar: A petabit photonic packet switch," IEEE J. Sel. Areas Commun., vol.21, no.7, pp.1096–1112, Sept. 2003.

[7] K.A. McCreer, "Arrayed waveguide gratings for wavelength routing," IEEE Commun. Mag., vol.36, no.12, pp.62–68, Dec. 1998.

[8] J. Ramamirtham, J. Turner, and J. Friedman, "Design of wavelength converting switches for optical burst switching," IEEE J. Sel. Areas Commun., vol.21, no.7, pp.1122–1132, Sept. 2003.

[9] A. Pattavina and R. Zanzottera, "Non-blocking WDM switches based on arrayed waveguide grating and shared wavelength conversion," Proc. IEEE INFOCOM 2006, Barcelona, Spain, April 2006.

[10] H.Q. Ngo, D. Pan, and C. Qiao, "Constructions and analyses of non-blocking WDM switches based on arrayed waveguide grating and limited wavelength conversion," IEEE/ACM Trans. Netw., vol.14, no.1, pp.205–217, Feb. 2006.

[11] C. Clos, "A study of nonblocking switching networks," Bell Syst. Tech. J., vol.32, pp.406–424, 1953.

[12] R.A. Spanke, "Architectures for guided-wave optical switching systems," IEEE Commun. Mag., vol.25, no.5, pp.42–48, 1987.

[13] T. Lin, K.A. Williams, R.V. Penty, L.H. White, M. Glick, and D. McAuley, "Performance and scalability of a single-stage SOA switch for  $10 \times 10$  Gb/s wavelength striped packet routing," IEEE Photonics Technol. Lett., vol.18, no.5, pp.691–693, March 2006.

[14] T. Lin, K.A. Williams, R.V. Penty, L.H. White, M. Glick, and D. McAuley, "Self-configuring intelligent control for short reach 100 Gb/s optical packet routing," Proc. OFC 2005, Paper OWK5, Anaheim, CA, March 2005.

[15] T.S. El-Bawab, Optical switching, Springer, 2006.

[16] H.Q. Ngo, D. Pan, and Y. Yang, "Optical switch networks with minimum number of limited-range wavelength converters," IEEE/ACM Trans. Netw., vol.15, no.4, pp.969–979, Aug. 2007.

[17] T.Y. Chai, T.H. Cheng, S.K. Bose, C. Lu, and G. Shen, "Crosstalk analysis for limited-wavelength-interchanging cross connects," IEEE Photonics Technol. Lett., vol.14, no.5, pp.696–698, May 2002.

[18] H. Takahashi, K. Oda, and H. Toba, "Impact of crosstalk in an arrayed-waveguide multiplexer on  $N \times N$  optical interconnection," J. Lightwave Technol., vol.14, no.6, pp.1097–1105, June 1996.

[19] Y. Shen, K. Lu, and W. Gu, "Coherent and incoherent crosstalk in WDM optical networks," J. Lightwave Technol., vol.17, no.5, pp.759–764, May 1999.

[20] T.Y. Chai, T.H. Cheng, Y. Ye, and Q. Liu, "Inband crosstalk analysis of optical cross-connect architectures," J. Lightwave Technol., vol.23, no.2, pp.688–701, Feb. 2005.

[21] R. Ramaswami and K.N. Sivarajan, Optical Networks — A Practical Perspective, Second ed., Morgan Kaufmann Publishers, 2001.

[22] J. Wei, Z. Min, and Y. PeiDa, "Novel analysis of cross-talk peculiarity of semiconductor optical amplifier switches based on cross-gain modulation in optical packet-switched networks," J. Opt. Soc. Am., vol.22, no.10, pp.2257–2262, Oct. 2005.

[23] S. Kamei, A. Kaneko, M. Ishii, T. Shibata, Y. Inoue, and Y. Hibino, "Crosstalk reduction in arrayed-waveguide grating multiplexer/demultiplexer using cascade connection," J. Lightwave Technol., vol.23, no.5, pp.1929–1938, May 2005.



**Yusuke Fukushima** received the B.S. degree from Department of Informatics of Yamagata University in 2004. He received the M.S. degree from Graduate School of Information Sciences, Tohoku University in 2006. He is currently studying for Ph.D. degree. His interests include interconnection networks and distributed systems.



**Xiaohong Jiang** received his B.S., M.S. and Ph.D. degrees in 1989, 1992, and 1999 respectively, all from Xidian University, Xi'an, China. He is currently an Associate Professor in the Department of Computer Science, Graduate School of Information Science, TOHOKU University, Japan. Before joining TOHOKU University, Dr. Jiang was an assistant professor in the Graduate School of Information Science, Japan Advanced Institute of Science and Technology (JAIST), from Oct. 2001 to Jan. 2005. Dr. Jiang was a

JSPS (Japan Society for the Promotion of Science) postdoctoral research fellow at JAIST from Oct. 1999–Oct. 2001. He was a research associate in the Department of Electronics and Electrical Engineering, the University of Edinburgh from March 1999–Oct. 1999. Dr. Jiang's research interests include optical switching networks, routers, network coding, WDM networks, VoIP, interconnection networks, IC yield modeling, timing analysis of digital circuits, clock distribution and fault-tolerant technologies for VLSI/WSI. He has published over 130 referred technical papers in these areas. He is a member of IEEE.



**Achille Pattavina** received the Dr.Eng. degree in Electronic Engineering from University "La Sapienza" of Rome (Italy) in 1977. He was with the same University until 1991 when he moved to "Politecnico di Milano," Milan (Italy), where he is now Full Professor. He has been author of more than 100 papers in the area of Communications Networks published in leading international journals and conference proceedings. He has been guest or co-guest editor of special issues on switching architectures in

IEEE and non-IEEE journals. He has been engaged in many research activities, including European Union funded projects. Dr. Pattavina has authored two books, *Switching Theory, Architectures and Performance in Broadband ATM Networks* (New York: Wiley, 1998) and *Communication Networks* (McGraw-Hill, 2002, in Italian). He has been Editor for Switching Architecture Performance of the *IEEE Transactions on Communications* since 1994 and Editor-in-Chief of the *European Transactions on Telecommunications* since 2001. He is a Senior Member of the IEEE Communications Society. His current research interests are in the area of optical networks and traffic modeling.



**Susumu Horiguchi** received the B.Eng the M.Eng. and Ph.D. degrees from Tohoku University in 1976, 1978 and 1981 respectively. He is currently a Full Professor in the Graduate School of Information Sciences, Tohoku University. He was a visiting scientist at the IBM Thomas J. Watson Research Center from 1986 to 1987. He was also a professor in the Graduate School of Information Science, JAIST (Japan Advanced Institute of Science and Technology).

He has been involved in organizing international workshops, symposia and conferences sponsored by the IEEE, IEICE, IASTED and IPS. He has published over 150 papers technical papers on optical networks, interconnection networks, parallel algorithms, high performance computer architectures and VLSI/WSI architectures. Prof. Horiguchi is members of IPS and IASTED.